ACCURATE NAVIGATION OF A UAV USING KALMAN FILTER BASED GPS / INS INTEGRATION

Anuj Sharma[1], **Puneet Kumar[1]**, Sushil Mohan Ratnaker[1], S E Talole[1]
[1]Scientist, Govt. of India
(puneetkumar.dce@gmail.com)

ABSTRACT

This paper presents work on navigation of a UAV by using Extended Kalman Filter based GPS / INS integration. A mathematical model has been developed and simulated for the same. A cruise trajectory at a fixed angle of attack is taken as the flight path of the UAV along with the assumption of ideal control. The UAV navigation is done using the Inertial Navigation System (INS) but the errors due to the INS measurements grow with time, which need to be checked. Thus GPS is used as another aid of measurement and is integrated with INS using Extended Kalman Filter to correct the INS state estimates. Also, the errors in accelerometer and gyroscope are estimated and are used to correct the accelerometer and gyroscope measurements to achieve a higher accuracy in navigation.

Key Words: Navigation, INS, GPS and Extended Kalman Filter

I. Introduction

Navigation is the art and science of maneuvering safely and efficiently from one point to another and there are varieties of means by which this may be achieved. A navigation system is required to provide an indication of the position of a vehicle with respect to a known reference frame.

Given the information about the vehicle's initial position, velocity and attitude and instantaneous accelerations and angular rates of the vehicle along the travelling path, the instantaneous position, velocity and attitude can be obtained by suitable integration of the resolved values of accelerations and angular rates in the reference frame. This navigation system is known as Inertial Navigation System (INS) [1, 4, 5, 6 and 7].

Inertial Measurement Unit (IMU) is the main component of the INS. Accelerometers and gyroscopes are the sensors in the IMU which measure linear accelerations and angular rates of the vehicle, respectively. However, the IMU measurements are erroneous due to the presence of random errors or unknown biases [1, 4, 5 and 6], which when integrated, lead to errors in the INS estimates of position, velocity and attitude. These errors grow with time, since they are added up always due to integration. Thus, these errors need to be checked for which some other instrument is required to correct the INS estimates time to time.

Global Positioning System (GPS) is a satellite based navigation system which is used to determine the position of a vehicle [1, 3, 4 and 5]. The GPS satellites send signals which are received by a GPS receiver. The signals contain information about the position of the GPS satellite and the time instant of transmission of the signal from the satellite. The time of arrival of the signal at the receiver is used to calculate the distance between the satellite and the receiver. Four such distances are used to determine the vehicle's position using trilateration method, taking into account the unknown time offset of the receiver's clock from the GPS system. The GPS itself is erroneous consisting of biases and zero-mean white noise errors [3 and 8]. The errors are due to clock offset of the receiver from the GPS system, ephemeris errors, signal propagation through ionosphere and troposphere, multipath of GPS signals and receiver noise errors [1, 3, 4, 5, 7 and 8]. The biases are due to the clock errors, ephemeris errors and atmospheric propagation errors [3 and 8]. The zero mean white noise is due to the multipath of GPS signals and the receiver's noise. The errors in GPS are instantaneous and do not grow with time.

GPS can be used to correct the INS estimates, as has been explained extensively in 1, 4, 5 and 7. Kalman Filter can be used to integrate the GPS and INS to increase the navigational accuracy in position, velocity and attitude.

Ref 4 demonstrates the integration of GPS and INS using Kalman Filter. It explains the propagation and correction of the errors in position, velocity and attitude by using the transition matrix dependent upon the true state estimates rather than the state estimates provided by the filter. This is not real, since in real life applications, such as aircraft or UAVs or missiles, the GPS / INS integration should be carried out with the transition matrix being dependent upon the filter state estimates. In this work, the full state of position, velocity and attitude is propagated using Extended Kalman Filter based integration of GPS / INS with the transition matrix being dependent upon the state estimates provided by the filter. Also, the estimation of biases in accelerometers and gyroscopes is carried out for increased accuracy in navigation.

---

[1]Scientist B, Aerial Delivery Research and Development Establishment, Agra, India
[2] Scientist B, Advanced Systems Laboratory, Hyderabad, India
[3]Scientist B, Aeronautical Development Establishment, Bangalore, India
[4]Scientist F, DIAT, Pune, India

The layout of this paper is as follows. Section II gives an overview of the work done. Section III explains the navigation using GPS / INS integration through block diagram representation. Sections IV and V describe the modelling of INS and GPS respectively. Section VI explains the integration of GPS and INS using Extended Kalman Filtering technique as has been modelled in this work. Section VII presents the entire modelling done in this work, in block diagram form. Section VIII presents the results of the Extended Kalman Filter based integration of GPS / INS for UAV navigation and the conclusions drawn from them.

II. Overview of the work done

This paper presents work on navigation of a UAV by using GPS / INS integration through Kalman Filter. Mathematical models have been developed and simulations have been done for the same. Point mass model of the UAV has been assumed and the navigation equations have been considered in the NED (local North, local East and local Down) frame, which is attached with the UAV. Spherical model of the earth has been considered. Low grade INS has been considered.

Position, velocity, attitude and the estimated accelerometer and gyroscope biases comprise the state vector. The position comprises latitude, longitude and altitude (height above the ground). The velocity comprises north, east and down velocities expressed in the NED frame. The attitude comprises roll, pitch and yaw angles (in radians) which represent the transformation from the NED to the body frame in the order yaw, pitch and roll. The estimated accelerometer and gyroscope biases comprise the estimated biases in accelerometer and gyroscope measurements in all three body axes.

A cruise flight at a speed of 60 m/sec at 5^o angle of attack at an altitude of 1 km for 2 hours duration along the constant 22.5^o longitude starting from 15^o latitude has been considered with the assumption of **ideal control**. Ideal control means that no control is modelled and that the flight path is maintained.

It is assumed that the axes of the accelerometers and gyroscopes are aligned with the body axes. Thus, the IMU measures accelerations and angular rates of the vehicle (with respect to the inertial frame) in the body frame. Fixed bias and zero mean white noise errors in gyroscopes and accelerometers have been considered in the IMU modelling. Markov process models have been considered for modelling the biases and white noise in the GPS signals. Extended Kalman Filtering technique has been used to integrate GPS and INS together into one system to be used for the UAV navigation.

The state vector estimation using INS is carried out at 100 Hz whereas the GPS measurement is taken at 1 Hz. Thus after every 100 propagations of the state vector, the state vector is corrected using the GPS measurement. In the absence of GPS signal, only INS data is used for navigation.

III. Block Diagram Representation of Navigation using GPS / INS Integration

Figure 1 portrays the Kalman Filter based GPS / INS integration in block diagram representation. It contains four main blocks namely IMU, Inertial Navigation System (INS), GPS and Kalman Filter.

The INS takes the state estimate at t_k, accelerations and angular rates, measured by the IMU, as inputs and integrates them in the respective frames to determine the position, velocity and attitude at the next time instant t_{k+1}. Thus, given the initial position, velocity and attitude of the system, the position, velocity and attitude at any time instant later on can be determined. The GPS measures the position of the vehicle. The Kalman Filter takes the INS state estimates and the GPS position measurements as inputs. It corrects the INS state estimates using the GPS position measurements. In this way, the navigation is carried out using GPS/ INS integration.

IV. Inertial Navigation System (INS)

INS has been used for the UAV navigation. The navigation equations have been considered in the NED frame (local North, local East and local Down frame) [4]. The north, east and down axes are considered as X, Y and Z axes respectively.

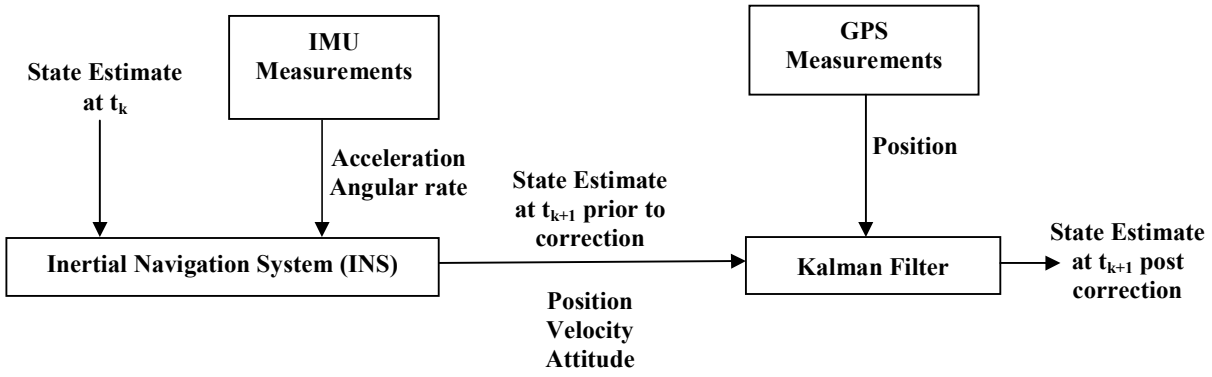

Figure 1: Block Diagram Representation of Navigation using GPS, INS and their integration

The state vector contains position, velocity, attitude and estimated accelerometer and gyroscope biases. The position is expressed in terms of latitude, longitude and altitude which are denoted as L, l and h respectively. The velocity is expressed in terms of North, East and Down velocities which are denoted as V_N, V_E and V_D respectively. The attitude is expressed in terms of Euler angles i.e. roll, pitch and yaw angles, which are denoted as ϕ, θ and ψ respectively. The Euler angles denote the transformation from NED frame to body frame in the order yaw, pitch and roll. The estimated accelerometer biases are represented as $acc_{bias,X}$, $acc_{bias,Y}$ and $acc_{bias,Z}$ respectively in all three body axes. Similarly, the estimated gyroscope biases are represented as $gyro_{bias,X}$, $gyro_{bias,Y}$ and $gyro_{bias,Z}$ respectively in all three body axes.

The state vector is expressed as follows:

$$X = [V_N \quad V_E \quad V_D \quad L \quad l \quad h \quad \phi \quad \theta \quad \psi \quad acc_{bias}^T \quad gyro_{bias}^T]^T \quad (1)$$

where, $acc_{bias} = [acc_{bias,X} \quad acc_{bias,Y} \quad acc_{bias,Z}]^T$ (2)

and $gyro_{bias} = [gyro_{bias,X} \quad gyro_{bias,Y} \quad gyro_{bias,Z}]^T$ (3)

The rate of change of position is expressed as follows [4]:

$$\begin{bmatrix} \dot{L} & \dot{l} & \dot{h} \end{bmatrix}^T = \begin{bmatrix} \frac{V_N}{R_e + h} & \frac{V_E \sec L}{R_e + h} & -V_D \end{bmatrix}^T \quad (4)$$

The rate of change of velocity is expressed as follows [4]:

$$\begin{pmatrix} \dot{V}_N \\ \dot{V}_E \\ \dot{V}_D \end{pmatrix} = \begin{pmatrix} f_N - 2\omega_e V_E \sin L + \frac{V_N V_D - V_E^2 \tan L}{R_e + h} - \frac{\omega_e^2 (R_e + h)}{2} \sin(2L) \\ f_E - 2\omega_e (V_N \sin L + V_D \cos L) + \frac{V_E}{R_e + h} (V_D + V_D \tan L) \\ f_D - 2\omega_e V_E \cos L - \frac{V_E^2 + V_N^2}{R_e + h} + g - \frac{\omega_e^2 (R_e + h)}{2} (1 + \cos(2L)) \end{pmatrix} \quad (5)$$

In the above equation, ω_e denotes the angular rate at which the earth spins about its axis; g denotes the acceleration due to gravity of the earth (assumed to be constant at all points on the earth; g: 9.8 m/sec^2) and f_N, f_E and f_D denote the forces acting on the body with respect to the inertial frame which are expressed in the NED frame. f_N, f_E and f_D can also be expressed as follows:

$$(f_N \quad f_E \quad f_D)^T = C_{b,NED}^T f_b^{F_b} \quad (6)$$

where $f_b^{F_b}$ is the force acting on the body with respect to the inertial frame and is expressed in the body frame.

The accelerometer measures $f_b^{F_b}$ as acceleration which is then transformed into the NED frame using equation 6. Since the accelerometer has biases, thus the accelerometer measurement is corrected using the estimated accelerometer bias as follows:

$$f_{b,corrected}^{F_b} = f_b^{F_b} - acc_{bias} \quad (7)$$

The rate of change of the Euler angles is expressed as follows [4]:

$$\begin{pmatrix} 1 & 0 & -\sin\theta \\ 0 & \cos\phi & \sin\phi\cos\theta \\ 0 & -\sin\phi & \cos\phi\cos\theta \end{pmatrix} \begin{pmatrix} \dot{\phi} \\ \dot{\theta} \\ \dot{\psi} \end{pmatrix} = \begin{pmatrix} p \\ q \\ r \end{pmatrix} \ldots$$
$$\ldots - C_{b,NED} \begin{pmatrix} \frac{V_E}{R_e + h} \\ -\frac{V_N}{R_e + h} \\ -\frac{V_E \tan L}{R_e + h} \end{pmatrix} - C_{b,NED} \begin{pmatrix} \omega_e \cos L \\ 0 \\ -\omega_e \sin L \end{pmatrix} \quad (8)$$

and p, q and r represent the angular rate at which the body rotates with respect to the inertial frame (expressed in the body frame) that is measured by the gyroscope. It is also denoted by $\omega_{b,I}^{F_b}$ and expressed as follows:

$$\omega_{b,I}^{F_b} = (p \quad q \quad r)^T \quad (9)$$

However, since the gyroscope has biases, the gyroscope measurement is corrected using the estimated gyroscope bias as follows:

$$\omega_{b,I,corrected}^{F_b} = \omega_{b,I}^{F_b} - gyro_{bias} \quad (10)$$

The rates of change of estimated velocity and attitude using the corrected accelerometer and gyroscope measurements as expressed in equations are expressed as follows:

$$\begin{pmatrix} \dot{V}_N \\ \dot{V}_E \\ \dot{V}_D \end{pmatrix} = C_{b,NED}^T \left(f_{b,corrected}^{F_b} \right) \ldots$$
$$\ldots + \begin{pmatrix} -2\omega_e V_E \sin L + \frac{V_N V_D - V_E^2 \tan L}{R_e + h} - \frac{\omega_e^2 (R_e + h)}{2} \sin(2L) \\ -2\omega_e (V_N \sin L + V_D \cos L) + \frac{V_E}{R_e + h} (V_D + V_D \tan L) \\ -2\omega_e V_E \cos L - \frac{V_E^2 + V_N^2}{R_e + h} + g - \frac{\omega_e^2 (R_e + h)}{2} (1 + \cos(2L)) \end{pmatrix} \quad (11)$$

$$\begin{pmatrix} 1 & 0 & -\sin\theta \\ 0 & \cos\phi & \sin\phi\cos\theta \\ 0 & -\sin\phi & \cos\phi\cos\theta \end{pmatrix} \begin{pmatrix} \dot{\phi} \\ \dot{\theta} \\ \dot{\psi} \end{pmatrix} = \omega_{b,I,corrected}^{F_b} \ldots$$
$$\ldots - C_{b,NED} \begin{pmatrix} \frac{V_E}{R_e + h} \\ -\frac{V_N}{R_e + h} \\ -\frac{V_E \tan L}{R_e + h} \end{pmatrix} - C_{b,NED} \begin{pmatrix} \omega_e \cos L \\ 0 \\ -\omega_e \sin L \end{pmatrix} \quad (12)$$

The rate of change of estimated accelerometer and gyroscope biases is taken as zero and is expressed as follows:

$$\dot{acc}_{bias} = [0 \quad 0 \quad 0]^T \tag{13}$$

and

$$\dot{gyro}_{bias} = [0 \quad 0 \quad 0]^T \tag{14}$$

The initial true, estimated and the errors in position, velocity, attitude and estimated accelerometer and gyroscope biases are considered as follows:

Parameters of the State Vector	True State Vector (X_0)	Estimated State Vector ($\hat{X}_0$)	Error in State Vector ΔX_0
North Velocity (V_N, m/sec)	60	40	20
East Velocity (V_E, m/sec)	0	40	40
Down Velocity (V_D, m/sec)	0	40	40
Latitude (L, deg)	15	15.1	0.1
Longitude (l, deg)	22.5	22.6	0.1
Altitude (h, m)	1000	2000	1000
Roll (deg)	0	10	10
Pitch (deg)	5	10	5
Yaw (deg)	0	10	10
Acc bias in X_b ($acc_{bias,X}$, m/sec^2)	0.001 g	0.0005 g	0.0005 g
Acc bias in Y_b ($acc_{bias,Y}$, m/sec^2)	0.001 g	0.0008 g	0.0002 g
Acc bias in Z_b ($acc_{bias,Z}$, m/sec^2)	0.001 g	0.0008 g	0.0002 g
Gyro bias in X_b ($gyro_{bias,X}$, deg/hr)	10	8	2
Gyro bias in Y_b ($gyro_{bias,Y}$, deg/hr)	10	5	5
Gyro bias in Z_b ($gyro_{bias,Z}$, deg/hr)	10	5	5

Table I: Initial True and Estimated States

The modelling of INS is carried out using the above equations. Low grade INS has been considered. Fixed bias and zero mean white noise errors have been considered in accelerometers and gyroscopes in the IMU modelling. The accelerometer and gyroscope biases are taken as 0.001 g and 10 deg / hr respectively in all three axes. The white noise in accelerometer and gyroscope is modelled by considering 9.6236 x 10^{-9} (m/sec^2)^2/Hz and 2.3504 x 10^{-13} (rad/sec)^2/Hz as white noise spectral density in accelerometer and gyroscope measurements.

The flight trajectory is chosen as mentioned in Section II. Thus, for the chosen flight, the rate of change of the state is expressed as:

$$\dot{X} = [0 \;\; 0 \;\; 0 \;\; \frac{V_N}{R_e + h} \;\; 0 \;\; 0 \;\; 0 \;\; 0 \;\; 0 \;\; 0 \;\; 0 \;\; 0 \;\; 0 \;\; 0 \;\; 0]^T \tag{15}$$

Since the initial true state is known, the true state at the next time instant can be determined by integrating the above equations. This process can be repeated at every time instant and the true state at the next time instant can be determined by integrating the above equations with the state being the current state. In this way, the true position, velocity and attitude of the UAV are determined throughout the flight.

Now, the modelling of IMU is explained in the following.

Using the values of the true state variables and their rates of change and putting them in equations 5 and 8, the true accelerations (f_N, f_E and f_D) and angular rates (p, q and r) are determined.

The acceleration of the body with respect to the inertial frame (expressed in the body frame), $f_b^{F_b}$ is determined by transforming f_N, f_E and f_D into the body frame using the roll, pitch and yaw angles using equation 6.

Now, fixed biases and zero mean white noise errors are added to $f_b^{F_b}$ and $\omega_{b,I}^{F_b}$ to simulate the measurement of accelerometers and gyroscopes. Thus,

$$f_{b,IMU}^{F_b} = f_b^{F_b} + bias_{acc}(1 \quad 1 \quad 1)^T + acc_{white} \tag{16}$$

$$\omega_{b,I,IMU}^{F_b} = \omega_{b,I}^{F_b} + bias_{gyro}(1 \quad 1 \quad 1)^T + gyro_{white} \tag{17}$$

where $bias_{acc} = 0.001\,g$ and $bias_{gyro} = 10\,\text{deg/}hr$ are accelerometer and gyroscope biases respectively. The white noise in accelerometer and gyroscope is considered as mentioned earlier in all the three body axes.

With the initial estimated state as mentioned in Table I, the IMU measurement at that instant is simulated using the above equations. Then the equations 11, 12, 13 and 14 are used to determine the rates of change of the estimated state at that instant. These rates are taken as constant over the time interval of 0.01 seconds and integrated over this interval to get the estimated state at the next time instant. This process is repeated for the estimated state at every time instant. In this way, the state estimation using INS is carried out.

V. Global Positioning System (GPS)

GPS has been used to correct the INS state estimates. GPS measurements are modelled at 1 Hz.

In real time GPS receivers, 4 of the visible satellites are selected for receiver's position determination. In this work, only 3 of the visible satellites are selected for position determination. It is so, because, no clock bias errors are considered in the modelling of GPS constellation signals. However, the clock bias errors are added to the true range measurements in order to simulate the GPS pseudorange measurements.

GPS constellation of 24 satellites, with their specifications as mentioned in Ref 9, is modelled and simulated using the satellite orbit modelling as mentioned in 1, 2 and 3.

The position of all the 24 satellites at every time instant during the entire flight is determined. The true state of the vehicle (as determined in Section IV) is used to determine the GPS satellites that are visible in the clear sky at that instant of time. Then the selection of the best configuration of the 3 GPS satellites that are to be selected for position determination is carried out by calculating the GDOP (Geometric Dilution of Precision) of all the possible 3 satellite configurations. The configuration with minimum

GDOP is selected for position determination [1, 3, 4, 5 and 7].

For modelling the real GPS measurements, errors are introduced in the GPS signals after the selection of the best configuration for position determination. The true distance between the GPS satellite (at the time of transmission of the signal) and the UAV (at the time of arrival of the signal) is determined using the true position of the vehicle and the position of the GPS satellite (determined using the modelling of GPS constellation). Now errors are added to this true range to make it pseudorange i.e. the range that would be measured between the satellite and the vehicle, if real GPS measurements would be considered.

The true ranges are expressed as follows:

$$\begin{pmatrix} R_1 \\ R_2 \\ R_3 \end{pmatrix} = \begin{pmatrix} \sqrt{(X_1 - X)^2 + (Y_1 - Y)^2 + (Z_1 - Z)^2} \\ \sqrt{(X_2 - X)^2 + (Y_2 - Y)^2 + (Z_2 - Z)^2} \\ \sqrt{(X_3 - X)^2 + (Y_3 - Y)^2 + (Z_3 - Z)^2} \end{pmatrix} \quad (18)$$

where (X_1, Y_1, Z_1), (X_2, Y_2, Z_2), (X_3, Y_3, Z_3) are the positions of the three satellites respectively and (X, Y, Z) is the position of the UAV. All the positions are expressed in Earth Centered Earth Fixed (ECEF) frame.

The position in ECEF frame is expressed in terms of latitude, longitude and altitude as follows:

$$\begin{pmatrix} X \\ Y \\ Z \end{pmatrix} = \begin{pmatrix} (R_e + h)\cos L \cos l \\ (R_e + h)\cos L \sin l \\ (R_e + h)\sin L \end{pmatrix} \quad (19)$$

The errors in GPS pseudorange measurements are considered to consist of bias and white noise as mentioned in Section I. The pseudorange measurement is denoted by z_k and is expressed as follows:

$$z_k = \text{true range} + b_k + v_k \quad (20)$$

where, b_k and v_k are bias and white noise respectively. Thus the pseudorange measurements are expressed as follows:

$$\begin{pmatrix} z_1 \\ z_2 \\ z_3 \end{pmatrix} = \begin{pmatrix} \sqrt{(X_1-X)^2+(Y_1-Y)^2+(Z_1-Z)^2} + b_1 + v_1 \\ \sqrt{(X_2-X)^2+(Y_2-Y)^2+(Z_2-Z)^2} + b_2 + v_2 \\ \sqrt{(X_3-X)^2+(Y_3-Y)^2+(Z_3-Z)^2} + b_3 + v_3 \end{pmatrix} \quad (21)$$

The biases and zero-mean white noises are considered as first-order exponentially correlated Markov process [3 and 8]. They are modelled as follows:

$$b_k = b_{k-1} \exp(-\beta_b \Delta t) + w_{b,k-1} \quad (22)$$

where, b_k is the discrete version of the bias at the time instant t_k and $1/\beta_b$ is the time constant of the process, Δt is the time interval at which the GPS measurements are simulated i.e. Δt is 1 second, $w_{b,k-1}$ is the discrete white noise process with variance equal to $q_b \Delta t$; q_b is the power spectral density of the continuous white noise of which $w_{b,k-1}$ is the discrete version, and $q_b = 2\sigma_b^2 \beta_b$, with σ_b^2 being the variance of the bias b_k. β_b and σ_b are taken as 1/750 sec^{-1} and 5.8 m respectively [8]. Similarly, the white noise in GPS pseudorange measurement has been modelled as Markov process with β_v and σ_v being 1/60 sec^{-1} and 1 m respectively [8].

VI. Extended Kalman Filter (EKF) based GPS / INS Integration

Extended Kalman Filter [1, 4, 5 and 7] is used to integrate two systems when the state of the system follows continuous state dynamics and the measurement of the second system is related to the estimates provided by the first system. The second system is used to correct the state estimates provided by the first system to yield an increased accuracy in state estimation.

The first and the second systems represent process and measurement models respectively. The state estimates and the measurements provided by the first and second systems are denoted by x and z respectively.

In this work, INS and GPS are considered as process and measurement models respectively. Extended Kalman Filter (EKF) has been used to integrate INS and GPS for an increased accuracy in UAV navigation. The terminology used in the present work is the same as mentioned in 1, 4, 5 and 7.

The state estimate at time t_k prior to correction is denoted by $\hat{x}_k^-$ and post correction is denoted by $\hat{x}_k^+$. The measurement by the second system at t_k is denoted by z_k.

The state propagation using INS is carried out as explained in Section IV. The state dynamics equations 11, 12, 13 and 14 are linearized with respect to the state estimates as mentioned below:

$$\begin{pmatrix} \Delta\dot{V}_N \\ \Delta\dot{V}_E \\ \Delta\dot{V}_D \end{pmatrix} = ([0_{3\times6} \quad -C_{b,NED}^T (f_{b,true}^{\times} - acc_{bias}^{\times}) \quad 0_{3\times6}])\Delta x \quad (23)$$
$$+ ([A \quad -C_{b,NED}^T \quad 0_{3\times3}])\Delta x + C_{b,NED}^T (\Delta f_{bias} + w_k)$$

$$\begin{pmatrix} \Delta\dot{L} \\ \Delta\dot{l} \\ \Delta\dot{h} \end{pmatrix} = \begin{pmatrix} \frac{1}{R_e+h} & 0 & 0 & 0 & 0 & -\frac{V_N}{(R_e+h)^2} & 0_{1\times9} \\ 0 & \frac{\sec L}{R_e+h} & 0 & \frac{V_E \sec L \tan L}{R_e+h} & 0 & -\frac{V_E \sec L}{(R_e+h)^2} & 0_{1\times9} \\ 0 & 0 & -1 & 0 & 0 & 0 & 0_{1\times9} \end{pmatrix} \Delta x \quad (24)$$

$$\begin{pmatrix} \Delta\dot{\phi} \\ \Delta\dot{\theta} \\ \Delta\dot{\psi} \end{pmatrix} = \left[\left[0_{3\times6} \quad A_1^{-1}A_2\right] + A_1^{-1}A_3 \quad 0_{3\times3} \quad -A_1^{-1}\right]\Delta x$$
$$+ A_1^{-1} \begin{pmatrix} \Delta p_{bias} \\ \Delta q_{bias} \\ \Delta r_{bias} \end{pmatrix} + A_1^{-1} \begin{pmatrix} \Delta p_{white} \\ \Delta q_{white} \\ \Delta r_{white} \end{pmatrix} \quad (25)$$

$$\begin{pmatrix} \Delta a\dot{c}c_{bias,X} \\ \Delta a\dot{c}c_{bias,Y} \\ \Delta a\dot{c}c_{bias,Z} \end{pmatrix} = \begin{pmatrix} 0 \\ 0 \\ 0 \end{pmatrix} \quad (26)$$

and

$$\begin{pmatrix} \Delta g\dot{y}ro_{bias,X} \\ \Delta g\dot{y}ro_{bias,Y} \\ \Delta g\dot{y}ro_{bias,Z} \end{pmatrix} = \begin{pmatrix} 0 \\ 0 \\ 0 \end{pmatrix} \quad (27)$$

Δf_{bias} and w_k are the bias and white noise in accelerometer measurements. Δp_{bias}, Δq_{bias} and Δr_{bias} are the biases in gyroscope measurements in roll, pitch and yaw axes respectively. Δp_{white}, Δq_{white} and Δr_{white} are the white noises in the gyroscope measurements in roll, pitch and yaw axes respectively.

The matrices A, A_1, A_2 and A_3 in equations 23 and 25 are expressed below. A_{ij} denotes the element at i^{th} row and j^{th} column in A. Similar convention is used to express the matrices A_1, A_2 and A_3.

$$A_{11} = \frac{V_D}{R_e + h} \quad (28)$$

$$A_{12} = -2\omega_e \sin L - \frac{2V_E \tan L}{R_e + h} \quad (29)$$

$$A_{13} = \frac{V_N}{R_e + h} \quad (30)$$

$$A_{14} = -2\omega_e V_E \cos L - \frac{V_E^2 \sec^2 L}{R_e + h} - \omega_e^2 (R_e + h)\cos(2L) \quad (31)$$

$$A_{15} = 0 \quad (32)$$

$$A_{16} = -\frac{V_N V_D}{(R_e + h)^2} - \frac{1}{2}\omega_e^2 \sin(2L) + \frac{V_E^2 \tan L}{(R_e + h)^2} \quad (33)$$

$$A_{17} = 0 \quad (34)$$

$$A_{18} = 0 \quad (35)$$

$$A_{19} = 0 \quad (36)$$

$$A_{21} = 2\omega_e \sin L + \frac{V_E \tan L}{R_e + h} \quad (37)$$

$$A_{22} = \frac{V_D}{R_e + h} + \frac{V_N \tan L}{R_e + h} \quad (38)$$

$$A_{23} = 2\omega_e \cos L + \frac{V_E}{R_e + h} \quad (39)$$

$$A_{24} = 2\omega_e V_N \cos L - 2\omega_e V_D \sin L + \frac{V_E V_N \sec^2 L}{R_e + h} \quad (40)$$

$$A_{25} = 0 \quad (41)$$

$$A_{26} = -\frac{V_E V_N \tan L}{(R_e + h)^2} - \frac{V_E V_D}{(R_e + h)^2} \quad (42)$$

$$A_{27} = 0 \quad (43)$$

$$A_{28} = 0 \quad (44)$$

$$A_{29} = 0 \quad (45)$$

$$A_{31} = -\frac{2V_N}{R_e + h} \quad (46)$$

$$A_{32} = -2\omega_e \cos L - \frac{2V_E}{R_e + h} \quad (47)$$

$$A_{33} = 0 \quad (48)$$

$$A_{34} = 2\omega_e V_E \sin L + \omega_e^2 (R_e + h)\sin(2L) \quad (49)$$

$$A_{35} = 0 \quad (50)$$

$$A_{36} = \frac{V_E^2}{(R_e + h)^2} + \frac{V_N^2}{(R_e + h)^2} - \frac{1}{2}\omega_e^2 (1 + \cos(2L)) \quad (51)$$

$$A_{37} = 0 \quad (52)$$

$$A_{38} = 0 \quad (53)$$

$$A_{39} = 0 \quad (54)$$

$$A_1 = \begin{pmatrix} 1 & 0 & -\sin\theta \\ 0 & \cos\phi & \sin\phi\cos\theta \\ 0 & -\sin\phi & \cos\phi\cos\theta \end{pmatrix} \quad (55)$$

$$A_2 = -\begin{pmatrix} 0 & -\dot{\psi}\cos\theta & 0 \\ -\dot{\theta}\sin\phi + \dot{\psi}\cos\phi\cos\theta & -\dot{\psi}\sin\phi\sin\theta & 0 \\ -\dot{\theta}\cos\phi - \dot{\psi}\sin\phi\cos\theta & -\dot{\psi}\cos\phi\sin\theta & 0 \end{pmatrix} \quad (56)$$

$$-(V')^{\times} - (\omega')^{\times}$$

where, $V' = C_{b,NED}\begin{pmatrix} \frac{V_E}{R_e + h} & -\frac{V_N}{R_e + h} & -\frac{V_E \tan L}{R_e + h} \end{pmatrix}^T$ (57)

and $\omega' = C_{b,NED}\begin{pmatrix} \omega_e \cos L & 0 & -\omega_e \sin L \end{pmatrix}^T$ (58)

and $\dot{\phi}, \dot{\theta}, \dot{\psi}$ are the Euler rates

where for any $B = [b_1 \quad b_2 \quad b_3]^T$, $B^{\times}$ is represented by the following expression:

$$B^{\times} = \begin{pmatrix} 0 & -b_3 & b_2 \\ b_3 & 0 & -b_1 \\ -b_2 & b_1 & 0 \end{pmatrix} \quad (59)$$

$$A_3 = -C_{b,NED}\begin{pmatrix} 0 & \frac{1}{R_e+h} & 0 & 0 & 0 & -\frac{V_E}{(R_e+h)^2} & 0_{1x3} \\ -\frac{1}{R_e+h} & 0 & 0 & 0 & 0 & \frac{V_N}{(R_e+h)^2} & 0_{1x3} \\ 0 & -\frac{\tan L}{R_e+h} & 0 & -\frac{V_E^2 \sec^2 L}{R_e+h} & 0 & \frac{V_E \tan L}{(R_e+h)^2} & 0_{1x3} \end{pmatrix} - C_{b,NED}\begin{pmatrix} 0_{1x3} & -\omega_e \sin L & 0_{1x5} \\ 0_{1x3} & 0 & 0_{1x5} \\ 0_{1x3} & -\omega_e \cos L & 0_{1x5} \end{pmatrix} \quad (60)$$

The linearization matrix that relates the rate of change of state error to the state error is expressed as follows:

$$F_k = \begin{pmatrix} F_{k,1to3,1to6} & F_{k,1to3,7to9} & F_{k,1to3,10to12} & F_{k,1to3,13to15} \\ & F_{k,4to6,1to6} & F_{k,4to6,7to15} & \\ & F_{k,7to9,1to15} & & \\ & F_{k,10to15,1to15} & & \end{pmatrix} \quad (61)$$

$$F_{k_{,1to3,1to6}} = \begin{bmatrix} A_{11} & A_{12} & A_{13} & A_{14} & A_{15} & A_{16} \\ A_{21} & A_{22} & A_{23} & A_{24} & A_{25} & A_{26} \\ A_{31} & A_{32} & A_{33} & A_{34} & A_{35} & A_{36} \end{bmatrix} \quad (62)$$

$$F_{k_{,1to3,7to9}} = \left[\begin{pmatrix} A_{17} & A_{18} & A_{19} \\ A_{27} & A_{28} & A_{29} \\ A_{37} & A_{38} & A_{39} \end{pmatrix} - C_{b,NED}^T (f_{b,IMU}^{\times} - acc_{bias}^{\times}) \right] \quad (63)$$

$$F_{k1to3,10to12} = -C_{b,NED}^T \quad (64)$$

$$F_{k1to3,13to15} = 0_{3\times3} \quad (65)$$

$$F_{k,4to6,1to6} = \begin{bmatrix} \frac{1}{R_e+h} & 0 & 0 & 0 & 0 & -\frac{V_N}{(R_e+h)^2} \\ 0 & \frac{\sec L}{R_e+h} & A_{53} & \frac{V_E \sec L \tan L}{R_e+h} & 0 & -\frac{V_E \sec L}{(R_e+h)^2} \\ 0 & 0 & -1 & 0 & 0 & 0 \end{bmatrix} \quad (66)$$

$$F_{k_{,4to6,7to15}} = 0_{3\times9} \quad (67)$$

$$(F_{k,7to9,1to15}) = ([0_{3\times6} \quad A_1^{-1}A_2] + A_1^{-1}A_3 \quad 0_{3\times3} \quad -A_1^{-1}) \quad (68)$$

and

$$F_{k,10to15,1to15} = 0_{6\times15} \quad (69)$$

The F_k matrix is determined using the equations 61 to 69 with the state estimates provided by the INS and the IMU measurements as modelled in Section IV. F_k is used to determine the transition matrix ϕ_k [1, 4, 5 and 7].

The process noise matrix Q_k as mentioned in 1, 4, 5 and 7 is determined using the following expressions for continuous process noise matrix Q and G (the linearization matrix obtained after linearizing the state dynamics equations with respect to the IMU measurements).

$$G = \begin{bmatrix} C_{b,NED}^T & 0_{3\times3} & 0_{3\times3} & 0_{3\times3} & 0_{3\times3} \\ 0_{3\times3} & I_{3\times3} & 0_{3\times3} & 0_{3\times3} & 0_{3\times3} \\ 0_{3\times3} & 0_{3\times3} & A_1^{-1} & 0_{3\times3} & 0_{3\times3} \\ 0_{3\times3} & 0_{3\times3} & 0_{3\times3} & I_{3\times3} & 0_{3\times3} \\ 0_{3\times3} & 0_{3\times3} & 0_{3\times3} & 0_{3\times3} & I_{3\times3} \end{bmatrix} \quad (70)$$

$$Q = \begin{bmatrix} n_{acc} I_{3\times3} & 0_{3\times3} & 0_{3\times3} & 0_{3\times3} & 0_{3\times3} \\ 0_{3\times3} & 0_{3\times3} & 0_{3\times3} & 0_{3\times3} & 0_{3\times3} \\ 0_{3\times3} & 0_{3\times3} & n_{gyro} I_{3\times3} & 0_{3\times3} & 0_{3\times3} \\ 0_{3\times3} & 0_{3\times3} & 0_{3\times3} & 0_{3\times3} & 0_{3\times3} \\ 0_{3\times3} & 0_{3\times3} & 0_{3\times3} & 0_{3\times3} & 0_{3\times3} \end{bmatrix} \quad (71)$$

where I_{3x3} is the 3x3 identity matrix and n_{acc} and n_{gyro} are the white noise spectral densities of accelerometer and gyroscope obtained after filter tuning for the convergence of state estimates to the true state.

The GPS pseudorange measurement z_k is determined using equation 21 with (X, Y, Z) being considered as the true position of the UAV.

For EKF based GPS / INS integration, the GPS measurement is also predicted using the state estimates provided by the INS. The estimated measurement at t_k is denoted by $\hat{z}_k$ and is determined using equation 18 where (X, Y, Z) is considered as the estimated position provided by the INS. The error in measurement prediction from the actual measurement, also known as innovation, is determined as follows:

$$\Delta z_k = z_k - \hat{z}_k \quad (72)$$

The linearization matrix H_k obtained after linearizing the pseudorange measurement with respect to the state vector is expressed as follows:

$$H_k = [0_{3\times3} \quad A_{4_{3\times3}} \quad 0_{3\times9}] \quad (73)$$

where

$$A_{4_{3\times3}} = A_5 \times A_6 \quad (74)$$

where

$$A_5 = \begin{pmatrix} -\frac{X_1 - X}{R_1} & -\frac{Y_1 - Y}{R_1} & -\frac{Z_1 - Z}{R_1} \\ -\frac{X_2 - X}{R_2} & -\frac{Y_2 - Y}{R_2} & -\frac{Z_2 - Z}{R_2} \\ -\frac{X_3 - X}{R_3} & -\frac{Y_3 - Y}{R_3} & -\frac{Z_3 - Z}{R_3} \end{pmatrix} \quad (75)$$

and

$$A_6 = \begin{pmatrix} -(R_e+h)\sin L \cos l & -(R_e+h)\cos L \sin l & \cos L \cos l \\ -(R_e+h)\sin L \sin l & (R_e+h)\cos L \cos l & \cos L \sin l \\ (R_e+h)\cos L & 0 & \sin L \end{pmatrix} \quad (76)$$

The GPS measurement noise matrix is determined using the Markov process models for bias and white noise in GPS as mentioned in Section V.

For an error modelled as Markov process, the variance of the error is expressed as follows [3 and 8]:

$$\sigma^2 = \sigma_b^2 (1 - e^{-2\beta_b \tau}) \quad (77)$$

Thus, the standard deviation of the white noise part of the GPS bias error $\sigma_{w,b}$ and GPS random error $\sigma_{w,b}$ is

modelled according to the equation 77 using the values as mentioned in Section V.

Thus the standard deviation in measurement noise is as expressed as follows:

$$\sigma_{pseudorange} = \sqrt{\sigma_{w,b}^2 + \sigma_{w,v}^2} = 6 \text{ meters} \quad (78)$$

and the measurement noise matrix is expressed as follows:

$$R_k = \begin{bmatrix} \sigma_{pseudorange}^2 & 0 & 0 \\ 0 & \sigma_{pseudorange}^2 & 0 \\ 0 & 0 & \sigma_{pseudorange}^2 \end{bmatrix} \quad (79)$$

The initial state error covariance P_0^- has been taken as follows:

$$P_0^- = \begin{pmatrix} \sigma_1 & 0 & 0 & 0 & 0 & 0 & 0 & 0 & 0 & 0 & 0 & 0 & 0 & 0 & 0 \\ 0 & \sigma_2 & 0 & 0 & 0 & 0 & 0 & 0 & 0 & 0 & 0 & 0 & 0 & 0 & 0 \\ 0 & 0 & \sigma_3 & 0 & 0 & 0 & 0 & 0 & 0 & 0 & 0 & 0 & 0 & 0 & 0 \\ 0 & 0 & 0 & \sigma_4 & 0 & 0 & 0 & 0 & 0 & 0 & 0 & 0 & 0 & 0 & 0 \\ 0 & 0 & 0 & 0 & \sigma_5 & 0 & 0 & 0 & 0 & 0 & 0 & 0 & 0 & 0 & 0 \\ 0 & 0 & 0 & 0 & 0 & \sigma_6 & 0 & 0 & 0 & 0 & 0 & 0 & 0 & 0 & 0 \\ 0 & 0 & 0 & 0 & 0 & 0 & \sigma_7 & 0 & 0 & 0 & 0 & 0 & 0 & 0 & 0 \\ 0 & 0 & 0 & 0 & 0 & 0 & 0 & \sigma_8 & 0 & 0 & 0 & 0 & 0 & 0 & 0 \\ 0 & 0 & 0 & 0 & 0 & 0 & 0 & 0 & \sigma_9 & 0 & 0 & 0 & 0 & 0 & 0 \\ 0 & 0 & 0 & 0 & 0 & 0 & 0 & 0 & 0 & \sigma_{10} & 0 & 0 & 0 & 0 & 0 \\ 0 & 0 & 0 & 0 & 0 & 0 & 0 & 0 & 0 & 0 & \sigma_{11} & 0 & 0 & 0 & 0 \\ 0 & 0 & 0 & 0 & 0 & 0 & 0 & 0 & 0 & 0 & 0 & \sigma_{12} & 0 & 0 & 0 \\ 0 & 0 & 0 & 0 & 0 & 0 & 0 & 0 & 0 & 0 & 0 & 0 & \sigma_{13} & 0 & 0 \\ 0 & 0 & 0 & 0 & 0 & 0 & 0 & 0 & 0 & 0 & 0 & 0 & 0 & \sigma_{14} & 0 \\ 0 & 0 & 0 & 0 & 0 & 0 & 0 & 0 & 0 & 0 & 0 & 0 & 0 & 0 & \sigma_{15} \end{pmatrix} \quad ....(80)$$

where the diagonal elements of P_0^- are expressed as follows:

$$\sigma_1 = \sigma_2 = \sigma_3 (10\ m/s)^2 \quad (81)$$

$$\sigma_4 = \sigma_5 = (0.001\ rad)^2 \quad (82)$$

$$\sigma_6 = (R_e \times 0.001\ m)^2 \quad (83)$$

$$\sigma_7 = \sigma_8 = \sigma_9 = (5\pi/180\ rad)^2 \quad (84)$$

$$\sigma_{10} = \sigma_{11} = \sigma_{12} = (0.0005 \times g)^2 \quad (85)$$

$$\sigma_{13} = \sigma_{14} = \sigma_{15} = (5\pi/(180 \times 3600))\ rad/s)^2 \quad (86)$$

i.e., 10 m/sec error has been considered in each of the north, east and down velocities estimation; 10^{-3} rad error has been considered in latitude and longitude estimation and the error in altitude estimation has been taken as R_e times 10^{-3} rad; and 5 deg error has been considered in each of the roll, pitch and yaw angles estimation; 0.0005 g bias error has been considered in each of the estimated accelerometer biases and 5 deg/hr error has been considered in the estimated gyroscope bias.

The state error covariance matrix P_k is propagated with time as mentioned in 1, 4, 5 and 7 to determine the state error covariance matrix prior to and post correction by GPS.

The Kalman Gain is determined using P_k, H_k and R_k as mentioned in 1, 4, 5 and 7 and is used along with the innovation to determine the required correction in the state estimate at t_k which is then used to correct the state estimate.

The Kalman Filter has been tuned at the following white noise power spectral densities for accelerometers and gyroscopes to obtain convergence of the state estimates to the true state of the UAV:

$$n_{acc} = 1 \times 10^{-5} \quad (87)$$

and

$$n_{gyro} = 1 \times 10^{-8} \quad (88)$$

VII. Overall Architecture of GPS / INS Integration using Extended Kalman Filter

Figure 2 represents the modelling of the Extended Kalman Filter based GPS / INS integration as explained in Sections III, IV, V and VI. It contains three main blocks namely Inertial Navigation System (INS), Global Positioning System (GPS) and Extended Kalman Filter.

The INS block takes as input the true state and estimated state of the UAV. It uses the true state to determine the rate of change of true state which is then used to determine the true accelerations and angular rates of the UAV. These true accelerations and angular rates are used to generate the IMU measurements by adding fixed biases and white noises to the true accelerations and angular rates as shown in the INS block. Next, the IMU measurements are used to determine the rate of change of INS state estimate, which is used to propagate the state estimate to the next time instant as shown in the INS block.

The GPS block takes the true state of the UAV as input, in particular, the position, which is used to model the GPS constellation. Also the satellites that are visible to the vehicle at that instant of time are determined. Next the selection of the 3 satellites to be used for position determination depending upon the minimum GDOP as mentioned in Section V is carried out. After the selection of the 3 satellites, the true ranges from each of the satellites to the UAV are determined. The true ranges are used to determine the pseudoranges by adding biases and white noises (that have been modelled as Markov processes) to the true ranges. In this way, the GPS measurements are modelled.

The EKF block takes as inputs the following: the state estimate prior to correction, the GPS pseudorange measurement and the positions of the 3 satellites considered for the UAV position determination in GPS modelling. The state estimate prior to correction is used to determine the predicted GPS true range measurement. The predicted true range and the pseudorange GPS measurements are used to determine the error in predicted GPS measurement. The Kalman Gain is determined and is used along with the error in GPS measurement prediction to determine the state estimate correction. This state estimate correction is added to the state estimate prior to correction to obtain the state estimate post correction. The updated state estimate is used to determine the transition matrix and the process noise covariance matrix which are used to propagate the state error covariance matrix to the next time instant of state estimation.

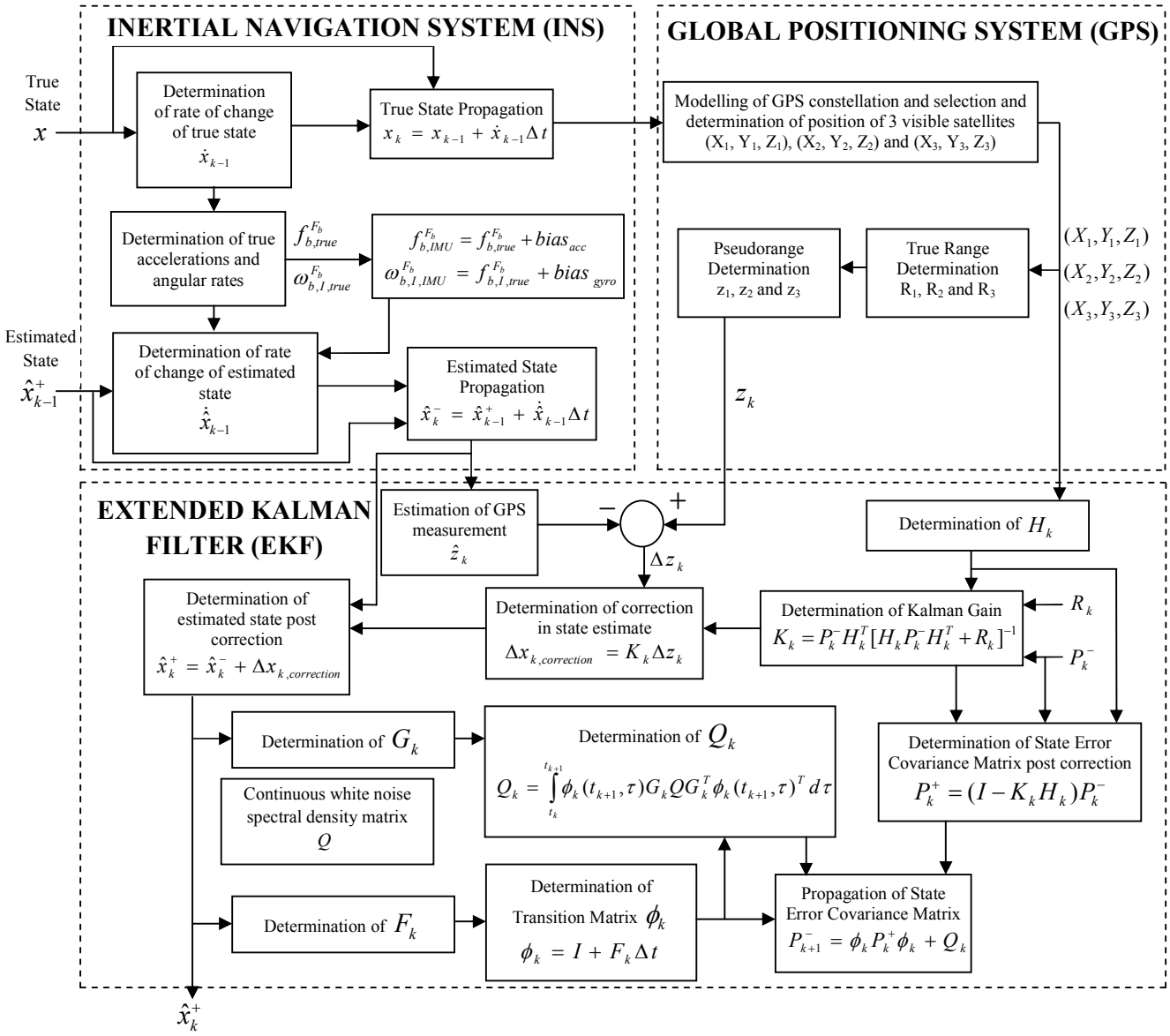

Figure 2: Block Diagram Representation of EKF based GPS/INS Integration for UAV Navigation

VIII. Results and Conclusions

The results of the mathematical modelling are shown in the following.

Figures 3, 4 and 5 represent the estimated velocity (north, east and down velocities), position (latitude, longitude and height) and attitude (roll, pitch and yaw angles) respectively. Figures 6, 7 and 8 represent the errors in the estimations of velocity, position and attitude respectively against ±3σ errors of filter estimation. Figure 9 represents the north and east position errors.

The conclusions of the results are discussed later in the paper.

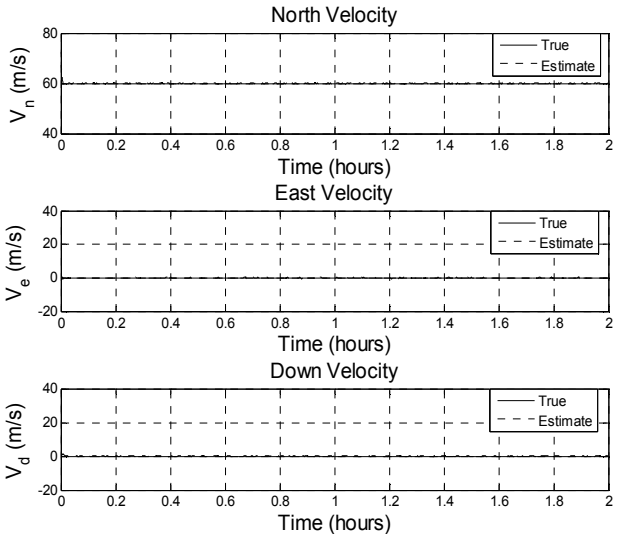

Figure 3: Velocity Estimation

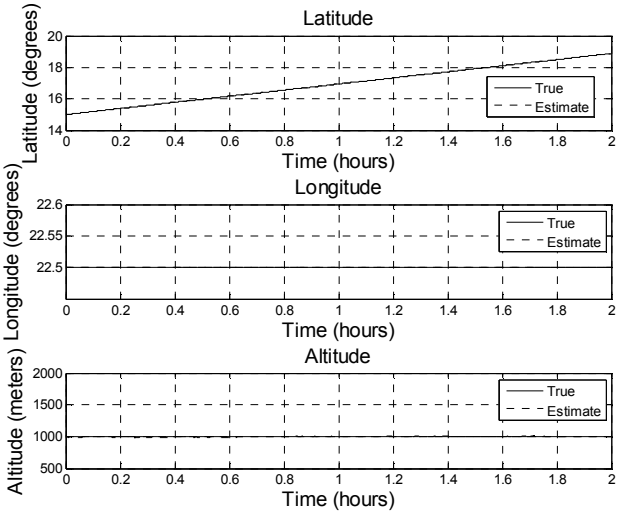

Figure 4: Position Estimation

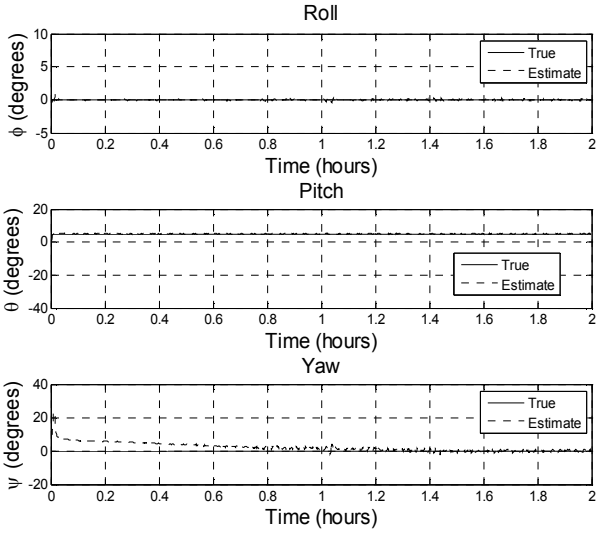

Figure 5: Attitude Estimation

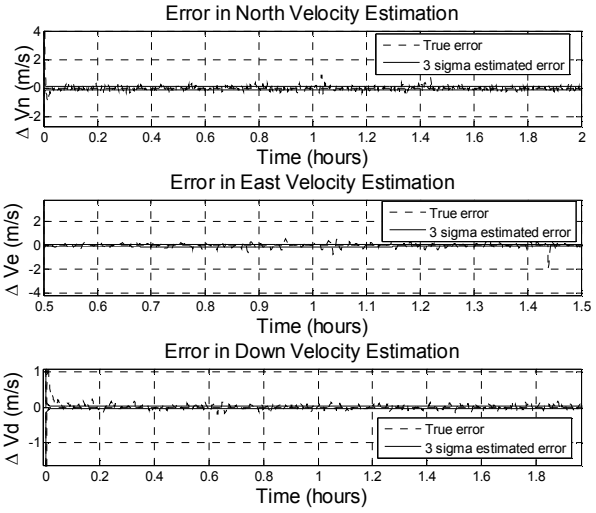

Figure 6: Error in Velocity Estimation

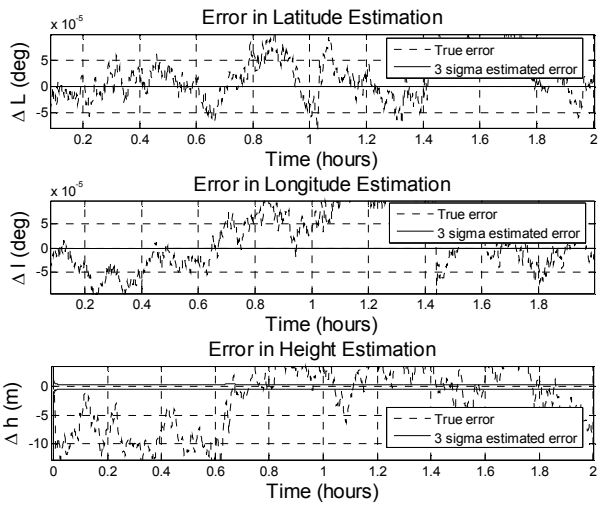

Figure 7: Error in Position Determination

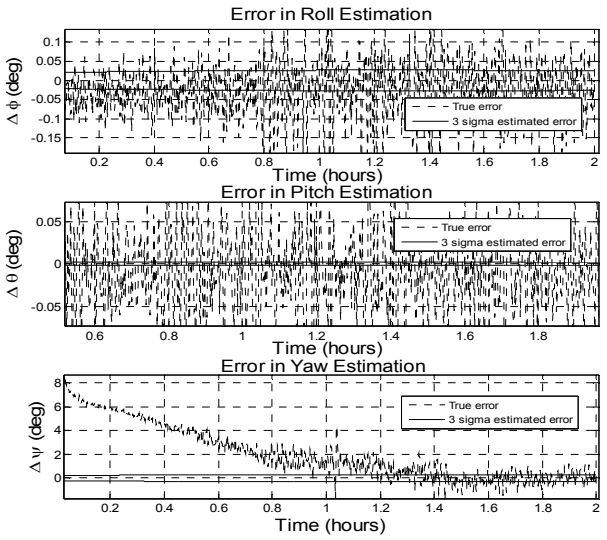

Figure 8: Error in Attitude Estimation

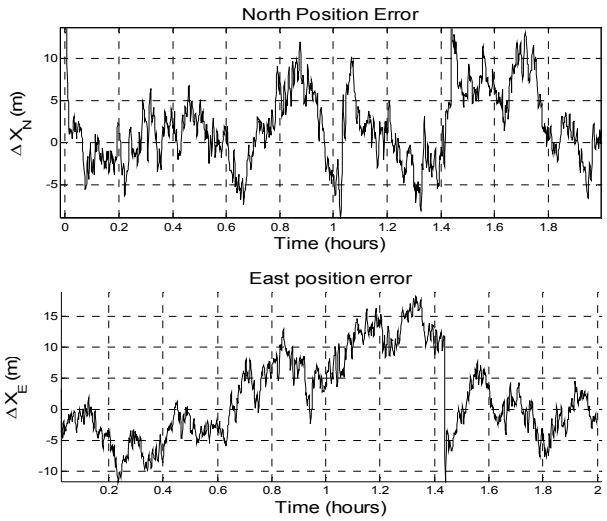

Figure 9: Error in North and East Position

Figures 3, 4 and 5 demonstrate the convergence of the estimates in velocity, position and attitude respectively to the true values.

Figure 6 demonstrates 0.2 m/sec error in velocity estimation in north, east and down directions and that the errors lie in ± 3σ errors predicted using Kalman Filtering.

Figure 7 demonstrates 15 x 10^{-5} rad error in latitude and longitude estimations. It also shows 15 m error in altitude estimations.

Figure 9 is another representation of latitude and longitude estimation accuracy in terms of errors in north and east position throughout the flight. It shows 15 m accuracy in north and east position estimation.

Figure 10 demonstrates 0.1 deg error in roll, pitch and yaw estimations. However, it is observed that the convergence in yaw estimations to the true yaw angle is slow in comparison to the convergence in estimations of roll and pitch to the true values in roll and pitch angles. Numerous values for accelerometer and gyroscope power spectral densities for filter tuning were tried out but still no better convergence in yaw was observed in comparison to the above results.

References

1. Grewal, Mohinder S., Weill, Lawrence R., Andrews, Angus P. (2007) : *Global Positioning Systems, Inertial Navigation, and Integration*, Second Edition, John Wiley & Sons, Ltd

2. Montenbruck, Oliver, Gill, Elberhard (2000) : *Satellite Orbits : Models, Methods and Applications*, Springer-Verlag

3. Misra, Pratap, Enge, Per (2006): *Global Positioning System : Signals, Measurements, and Performance*, Second Edition, Ganga-Jamuna Press.

4. Titterton, D. H., Weston, J. L. (2004): *Strapdown Inertial Navigation Technology*, Second Edition, AIAA.

5. Biezad, Daniel J. (1999): *Integrated Navigation and Guidance Systems*, AIAA Education Series.

6. Stevens, Brian L., Lewis, Frank L. (2003): *Aircraft Control and Simulation*, Second Edition, John Wiley & Sons, Inc.

7. Shalom, Yaakov Bar, Li, X. Rong, Kirubarajan, Thiagalingam: *Estimation with Applications to Tracking and Navigation*.

8. Hablani, Hari B., (2009), 'Autonomous Inertial Relative Navigation with Sight-Line-Stabilized Integrated Sensors for Spacecraft Rendezvous', Journal of Guidance, Control, and Dynamics, Vol. 32, No.1, January-February, 2009.

9. Dierendonck, Dr. A J Van, 'Current GPS Constellation', A J Systems.